Robotica (2025), **43**, pp. 4040–4063
doi:10.1017/S0263574725102762

CAMBRIDGE UNIVERSITY PRESS

RESEARCH ARTICLE

On the force-pose stability sensitivity analysis method for six-degree-of-freedom spatial cable-suspended parallel robots with eight cables

Peng Liu[1,2], Xuechao Duan[2], Zhufeng Shao[3] and Jing Xia[1]

[1]Shaanxi Key Laboratory of Mine Electromechanical Equipment Intelligent Detection and Control, Xi'an University of Science and Technology, Xi'an, 710054, China
[2]Key Laboratory of Ministry of Education for Electronic Equipment Structure Design, Xidian University, Xi'an, 710000, China
[3]State Key Laboratory of Tribology, Department of Mechanical Engineering, Tsinghua University, Beijing, 100084, China
Corresponding author: Peng Liu; Emails: liupeng@xust.edu.cn; 200304405liupeng@163.com

Received: 4 January 2025; **Revised:** 6 August 2025; **Accepted:** 27 September 2025;
First published online: 18 November 2025

Keywords: cable-suspended parallel robot; stability; force-pose; sensitivity

Abstract

This paper focuses on six-degree-of-freedom (six-DOF) spatial cable-suspended parallel robots with eight cables (8-6 CSPRs) because the redundantly actuated CSPRs are relevant in many applications, such as large-scale assembly and handling tasks, and pick-and-place operations. One of the main concerns for the 8-6 CSPRs is the stability because employing cables with strong flexibility and unidirectional restraint operates the end-effector of the robot under external disturbances. As a consequence, this paper attempts to address two key issues related to the 8-6 CSPRs: the force-pose stability measure method and the stability sensitivity analysis method. First, a force-pose stability measure model taking into account the poses of the end-effector and the cable tensions of the 8-6 CSPR is presented, in which two cable tension influencing factors and two position influencing factors are developed, while an attitude influence function representing the influence of the attitudes of the end-effector on the stability of the robot is constructed. And furthermore, a new type of workspace related to the force-pose stability of the 8-6 CSPRs is defined and generated in this paper. Second, a force-pose stability sensitivity analysis method for the 8-6 CSPRs is developed with the gray relational analysis method, where the relationship between the force-pose stability of the robot and the 14 influencing factors (the end-effector's poses and cable tensions) is investigated to reveal the sequence of the 14 influencing factors on the force-pose stability of the robot. Finally, the proposed force-pose stability measure method and stability sensitivity analysis method for the 8-6 CSPRs are verified through simulations.

1. Introduction

1.1. Background and motivation

Cable-driven parallel robots have advantages over their rigid-link counterparts, such as simple lightweight mechanical structure and large reachable workspace [1–4]. As a result, the cable-driven parallel robots become a current study in the field of engineering such as medical rehabilitation [5–6], wind tunnel experiment [7], astronomical observation [8], and 3D printing [9–10]. It is well known that increasing the number of cables can improve the performance of cable-driven parallel robots in terms of workspace extension and payload capability under specific conditions where lower cable tension constraints are satisfied to prevent slackness of the cables. However, this potential benefit must be balanced against the increased likelihood of the interferences between cables and the end-effector that arises with additional cables. It should be noted that cable-suspended parallel robots are more appropriate for pick-and-place operations and large-scale assembly and handling tasks because of smaller possibility of cable

© The Author(s), 2025. Published by Cambridge University Press.

https://doi.org/10.1017/S0263574725102762 Published online by Cambridge University Press

collisions and interferences, as well as less payload swing in contrary to classical cranes. The six-degree-of-freedom (six-DOF) cable-suspended parallel robots driven by eight cables have been employed in the field of the pick-and-place operations of large and heavy parts [11]. Consequently, this paper focuses on a particular type of cable-driven parallel robot, namely a six-DOF cable-suspended parallel robots with eight cables (8-6 CSPR). To the best of the authors' knowledge, one of the most important issues in the 8-6 CSPRs is that of the stability of the robot because employing cables with strong flexibility and unidirectional restraint operates the end-effector of the robot under external disturbances. As a matter of fact, the stability of the 8-6 CSPRs indicates the ability of robot to resist external interferences in the weakest constraint direction and to make the end-effector of the 8-6 CSPR be in equilibrium with external disturbances. In this regard, there are two key challenges in the theoretical research and application of the 8-6 CSPRs:

(i) For one thing, the strong coupling effect between the cable-driven system and the end-effector makes it difficult to establish a stability measure model for 8-6 CSPRs. On the one hand, the inherent strong flexibility and unidirectional constraints of the employed cables make it difficult to maintain the stability of the 8-6 CSPRs. On the other hand, the end-effector of the 8-6 CSPRs is driven by eight cables, and thus, the cable-driven system has an important effect on the stability of the robot; vice versa, the poses of the end-effector will inevitably affect the stability of the cable-driven system.

(ii) And for another, considerable number of influencing factors and extremely complicated influencing mechanism on the stability of the 8-6 CSPRs makes it difficult to investigate importance ordering of these influencing factors on the stability of the 8-6 CSPRs. It should be noted that the stability of the 8-6 CSPRs can be affected by a total of 14 influencing factors, such as the cable tensions, end-effector's positions, and end-effector's attitudes. And furthermore, the influence degree of each influencing factor on the stability of the 8-6 CSPRs is different. As a result, the complicated influencing mechanism of the 14 influencing factors on the stability of the 8-6 CSPRs has brought severe challenges to establishing a stability sensitivity analysis model for the robots.

As a consequence, two main issues related to 8-6 CSPRs are discussed in this paper: force-pose stability measures and stability sensitivity analysis. The force-pose stability measures aims to evaluate the robot's ability to resist external disturbances applied to the end-effector of the 8-6 CSPRs, while the stability sensitivity analysis aims to investigate the importance of influencing factors for the stability of the robots.

1.2. Literature review and comments

The use of cables introduces many new challenges, and indeed, the stability issues are particularly important and critical for the cable-driven parallel robots. It is extremely important to measure and ensure the stability of the cable-driven parallel robots. The existing literature, however, does not adequately address these issues. As a result, we briefly review the literature reporting the stability of the cable-driven parallel robots from two aspects in this section. The domestic and international researches on reporting the stability measure method for the cable-driven parallel robots are presented. Meanwhile, the literature related to the stability sensitivity analysis method for the robots is investigated in this paper.

On the one hand, one of the fundamental issues is the stability of the 8-6 CSPRs under external disturbances, and stability measures and stability evaluation methods for the robots have been a topic of interest. In fact, the stability is an important prerequisite for the control of the robots. In order to assess the quality of the stability of the 8-6 CSPRs for a particular pose or configuration, it becomes necessary to define stability measure indices. Stability measures and stability evaluation are a key and challenging problem in both the theory and application of the 8-6 CSPRs. In recent years, several related studies have been conducted to the stability of the cable-driven parallel robots. Behzadipour et al. [12] presented a new approach to derive the total stiffness that is used to evaluate the stability of the cable-driven parallel robot. Liu et al. [13] investigated the minimum cable tension distributions in the workspace for the

https://doi.org/10.1017/S0263574725102762 Published online by Cambridge University Press

cable-driven parallel robot, and furthermore, the relationship between the stability and the minimum cable tensions is explained to a certain degree. But they missed a key step, that is, to mathematically show the relationship between them. Indeed, these literatures just regard the stability of the cable-driven parallel robots as two states, a stable state and a nonstable one. To address these issues, researchers have proposed a few of stability measure indices for the cable-driven parallel robots. Bosscher et al. [14–15] investigated a slope-based robustness measure for underconstrained cable-driven parallel robot, which can employ the quantifiable numbers to measure the robot's stability. In another paper, an approach to investigate the stability of the cable-driven camera robot quantitatively was proposed in our preliminary work [16], and the main innovation of this work is extending the stability of the cable-driven parallel robots from the binary state to the interval [0,1]. Based on ref. [16], Wei et al. [17] focused on the effect of cable tensions and stiffness on the stability for the camera robot driven by four cables with the proposed tension factors and stiffness factors. Wang et al. [18] reported a stability index for a lower-limb rehabilitation training robot driven by cables. To the best of the authors' knowledge, ref. [19] is the most recent work on the cable-driven parallel robot dealing with measuring the stability of the robots. However, all these previous works only investigate the effects of the positions of the end-effector, cable tensions, and stiffness on the stability of the robots where the important influencing factor such as the attitudes of the end-effector not taken into account. And furthermore, to the authors' best knowledge, one way to address this issue is to propose an attitude influence function (AIF) that represents the effects of end-effector's attitudes on the stability of the cable-driven parallel robots. As a consequence, a systematic method on the stability for the 8-6 CSPRs with combination of cable tensions and end-effector's poses presented herein seeks to fill this gap.

On the other hand, another critical concern is the stability sensitivity analysis model, through which the influence degree of each influencing factor on the stability of the robot can be obtained and, their sequence can be ranked with their importance degrees. Nevertheless, the stability mechanism for the cable-driven parallel robots is extremely complicated and affected by considerable number of factors, for example, cable tensions, end-effector's positions, and end-effector's attitudes. Actually, the influence degree of the above influencing factors on the stability of the cable-driven parallel robots, as far as I am concerned, can be reflected using stability sensitivity, and furthermore, their sequence can be ranked with the importance of each influencing factor. It should be noted that, to the best of our knowledge, few studies find that the stability sensitivity for the cable-driven parallel robots is addressed, especially for the 8-6 CSPRs where the effects of the end-effector's attitudes on the stability of the robots have to be considered in this case. Several approaches have been proposed in the literature for the investigation of the importance of influencing factors on the stability for the cable-driven parallel robots. To our knowledge, the first approach for investigating the stability sensitivity analysis for the cable-driven parallel robots is proposed in ref. [20], in which a method to quantitatively assess the stability sensitivity for a coal-gangue sorting cable robot is proposed. In another paper, two special problems of carrying out dynamic stability measurement and a stability sensitivity analysis for the high-speed long-span 4-1 cable-driven parallel robots are reported in ref. [21]. In addition, in our previous study [22], a stability measure method and a stability sensitivity evaluation model for camera robots while considering the cable mass and sags are presented. It can be seen that the gray relational analysis method can describe the relationships between the main factors and all the other factors [23–26], and therefore, it can be employed to obtain the sensitivity of each influencing factor and rank their sequences. As a matter of fact, there are multiple factors which can influence the stability of the 8-6 CSPRs, such as the cable tensions, the positions, and the attitudes of the end-effector. This paper, as a result, is to develop a method for force-pose stability sensitivity analysis for the 8-6 CSPRs. And furthermore, the most sensitive factor among the stability influencing factors can be identified and prioritized.

To sum up, it should be pointed out that the stability of the 8-6 CSPRs considering the effects of the attitudes of the end-effector has not been considered in previous studies. Additionally, to the authors' best knowledge, the relationship between the stability of the robot and their influencing factors has not been investigated up to now. Therefore, this paper attempts to address two key issues related to the 8-6 CSPR: the force-pose stability measure method and the stability sensitivity analysis method. In addition, it is

https://doi.org/10.1017/S0263574725102762 Published online by Cambridge University Press

worth noting that the main advantage of the proposed force-pose stability measure method and stability sensitivity analysis method for the 8-6 CSPRs lies in its ability to explicitly investigate the effects of the poses of the end-effector and cable tensions on the stability of the robots.

1.3. Contribution and paper organization

Considering the above-mentioned previous work, this paper aims to extend the force-position measure approach on the stability for a camera robot being a CDPR with a point-mass end-effector proposed in refs. [16, 20, 22] by developing, for the first time, an AIF to emphasize the effects of the end-effector's attitudes on the stability of CDPRs. Therefore, the most scientific contribution and innovation of this paper, compared with the existing literature, can be highlighted as follows:

(i) To the best of our knowledge, this is the first time that the effects of the end-effector's poses and cable tensions on the stability of the 8-6 CSPRs are investigated, and further, a force-pose stability measure method for the 8-6 CSPR is developed. The work in this paper is also an extension of the preliminary study on the stability of the cable-driven parallel robots in ref. [16], and the novelty of the proposed force-pose stability measure method for the robot includes considering the effects of the attitudes of the end-effector on the stability of the robot.

(ii) Meanwhile the main contribution of this paper, as far as the authors know, is that a force-pose stability sensitivity analysis method for the 8-6 CSPR is presented with the gray correlation analysis method. Compared with the refs. [20, 22], this paper emphatically investigates the effects of the end-effector's attitudes on the stability of the robot, and furthermore, the sequence of the 14 influencing factors on the force-pose stability of the robot is revealed.

This paper is organized as follows. The next section presents the proposed stability influencing factors. Subsequently, a force-pose stability measure method to the 8-6 CSPR is developed in Section 3. In addition, a force-pose stability sensitivity analysis method for the 8-6 CSPR is proposed in Section 4. Furthermore, the presented methods on the force-pose stability measures and stability sensitivity analysis for the 8-6 CSPR are explained through simulation results in Section 5. Finally, Section 6 concludes this paper and discusses the contributions and presents possibilities for future continuations of this work.

2. The stability influencing factors

This work focuses the investigation on the class of cable-suspended parallel robots with six-DOF driven by eight cables (8-6 CSPRs). Due to the unilateral driving property of the used cables, maintaining positive cable tension is necessary condition of the stability while the end-effector locates at a given equilibrium pose for the 8-6 CSPRs. And furthermore, the cable possessing the minimum cable tension may be slack when the minimum cable tension is less than a certain value, leading to missing the ability to control the end-effector of the 8-6 CSPRs. Therefore, the minimum cable tension satisfying certain condition is required to make the end-effector to be stable while the end-effector locates at a given equilibrium pose. It can be inferred that the stability of the 8-6 CSPRs is associated with a particular pose where a family of cable tensions is required to make the end-effector to be in equilibrium. Therefore, both the end-effector's poses and cable tensions have important effects on the stability of the 8-6 CSPRs. This paper aims at highlighting the effects of the end-effector's poses and cable tensions on the stability of the 8-6 CSPRs. And furthermore, special attention should be paid to the fact that the positions and the attitudes of the end-effector, from the point of view of the robot kinematics, are independent mutually, leading to having independent effects on the stability of the 8-6 CSPRs. As a result, this section, prior to the detailed description of the proposed force-pose stability for the 8-6 CSPRs, is devoted to introduce main influencing factors on the stability of the robots, including two position influencing factors (PIFs), two cable tension influencing factors (CTIFs), and an AIF.

https://doi.org/10.1017/S0263574725102762 Published online by Cambridge University Press

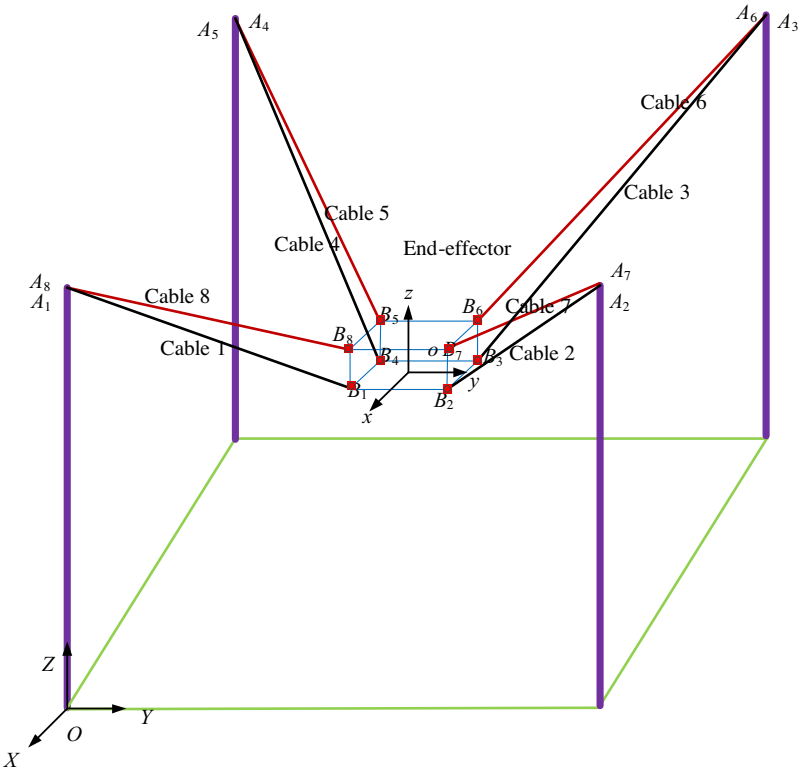


Figure 1. *The investigated 8-6 CSPR.*

2.1. Position influencing factor (PIF)

Prior to the detailed description of the proposed influencing factors on the stability of the 8-6 CSPRs and the force-pose stability measure method, this section first introduces kinematics, static equilibrium equation, and the distributions of cable tensions for the 8-6 CSPRs. In the following analysis, the following assumptions are made in this paper: (i) the mass and the elasticity of the employed cables are negligible; (ii) the end-effector of the investigated 8-6 CSPR is assumed to be a rigid body; and (iii) and the employed cable is considered to be a straight segment. And these assumptions are reasonable in several CSPRs.

The six-DOF cable-suspended parallel robot with eight cables (8-6 CSPR) investigated in this paper is represented in Fig. 1. It consists of an end-effector connected to the base by a set of eight cables and to fixed pulleys where the employed cables are wound. Note that the end-effector of the robot refers to the whole mobile platform, including the employed tool for pick-and-place operations. In this regard, the position and orientation of the end-effector can be controlled by changing the eight cable's lengths, respectively. Referring to Fig. 1, the notation employed in the section is as follows: a fixed reference frame, noted by *O-XYZ*, is attached to the base of the 8-6 CSPR and is referred to as the base frame. And a moving reference frame, noted by *o-xyz*, is attached to the end-effector of the robot, where o is the reference point to be positioned at the end-effector. Point A_i, where the ith cable ($i = 1, 2, \ldots, 8$) enters its spool, is assumed to be fixed relative to the base. Furthermore, the ith cable is attached at point B_i on the end-effector, and this attachment point is assumed to be fixed relative to the end-effector of the 8-6 CSPR. The ith cable then connects points A_i and B_i, and its length is denoted as ρ_i. The contact points A_i and B_i are modeled as spherical joints. Then, vectors $\boldsymbol{a}_i$ and $\boldsymbol{b}_i$ are defined as the vectors connecting point O to point A_i and point o to point B_i, expressed in the base frame and the moving reference frame, respectively.

https://doi.org/10.1017/S0263574725102762 Published online by Cambridge University Press

In this regard, the end-effector's position of the 8-6 CSPR is given by the vector $\boldsymbol{P} = [x, y, z]^{\mathrm{T}}$ connecting point O to point o, while the orientation of the end-effector, given by a space-three rotation sequence of ϕ about X, θ about Y, and ψ about Z, is denoted by $\alpha = [\phi, \theta, \psi]^{\mathrm{T}}$. As a result, the end-effector's pose of the 8-6 CSPR can be given by the vector $X = [x, y, z, \phi, \theta, \psi]^{\mathrm{T}}$. By simple geometrical considerations in Fig. 1, the unit vector depending on the pose of the end-effector along cable i is noted by $\boldsymbol{d}_i$ and can be written as:

$$\boldsymbol{d}_i = \left(\boldsymbol{a}_i - {}^{O}\boldsymbol{R}_o\boldsymbol{b}_i - \boldsymbol{P}\right)/\rho_i, i = 1,2,\ldots,8 \tag{1}$$

$$\rho_i = \left\|\boldsymbol{a}_i - {}^{O}\boldsymbol{R}_o\boldsymbol{b}_i - \boldsymbol{P}\right\|_2 \tag{2}$$

where $\|\cdot\|_2$ denotes the Euclidean norm of the vector argument and ${}^{O}\boldsymbol{R}_o$ represents the rotation matrix of the moving frame with respect to the base frame, and it can be written as follows:

$${}^{O}\boldsymbol{R}_o = \begin{bmatrix} \cos\psi\cos\theta & \cos\psi\sin\theta\sin\phi - \sin\psi\cos\phi & \cos\psi\sin\theta\cos\phi + \sin\psi\sin\phi \\ \sin\psi\cos\theta & \sin\psi\sin\theta\sin\phi + \cos\psi\cos\phi & \sin\psi\sin\theta\cos\phi - \cos\psi\sin\phi \\ -\sin\theta & \cos\theta\sin\phi & \cos\theta\cos\phi \end{bmatrix} \tag{3}$$

As mentioned before, both the end-effector's poses and cable tensions have important effects on the stability of the 8-6 CSPRs. The stability of the robots, in other words, is pose-dependent and tension-dependent. Indeed, it is well known that the motion of the end-effector of the 8-6 CSPR can be simplified as the superposition of the translation of the center of the end-effector's mass and the rotation around the center of the end-effector's mass. As a result, the positions and the attitudes of the end-effector, from the point of view of the robot kinematics, are mutually decoupled and do not affect each other, and therefore, their influences on the stability of the robots can be considered separately. It is noted that the attitude of the end-effector is described with the rotation matrix ${}^{O}\boldsymbol{R}_o$ in this paper, and it is a crucial aspect of the end-effector's pose of the 8-6 CSPR, which also includes its position. In this regard, two PIFs, two CTIFs, and an AIF are proposed in this paper. First of all, this section deals mainly with the effects of the end-effector's positions and cable tensions on the stability of 8-6 CSPRs. Previous work has considered both the effects of the end-effector's positions and cable tensions on the stability of robots, and therefore, for a detailed description of the two PIFs and the two CTIFs, the reader is referred to ref. [16]. Some results of the foregoing references are provided in what follows.

Consequently, two PIFs and two CTIFs are discussed in more detail based on kinematics and cable tension distributions of the 8-6 CSPR; moreover, the schematic diagram relating to the PIFs and CTIFs is shown in Fig. 2. It should be pointed out that among the eight cables for the 8-6 CSPR, the cable with the minimum cable tension has an important influence on maintaining the stability of the end-effector, while the end-effector of the 8-6 CSPR is located at arbitrary pose within the workspace, because this is the weakest constraint direction for the end-effector of the robot. And the minimum cable tension denoted by $T_{\min}$ while the end-effector of the 8-6 CSPR is located at arbitrary pose within the workspace can be obtained with the determination of the cable tension distributions, and it will be investigated in the next section. The optional position of the end-effector for the 8-6 CSPR in the workspace is denoted by P; the geometric vertical midline of the workspace for the 8-6 CSPR when the end-effector's orientation is fixed as (0, 0, 0) is denoted by a; the horizontal plane where the specified position of the end-effector is located is highlighted with the green; the intersection between the presented geometric vertical midline and the given horizontal plane is denoted by Q; the top intersection between the presented geometric vertical midline and the workspace of the robot is denoted by M; the minimum cable tensions when the end-effector of 8-6 CSPRs locates at the positions P, Q, and M are denoted by $T_{P,\min}$, $T_{Q,\min}$, and $T_{M,\min}$, respectively; the angles between the cable having the minimum cable tension and the horizontal plane when the end-effector of the 8-6 CSPR is located at the positions P, Q, and M are denoted by α_P, α_Q and α_M, respectively.

In more detail, two PIFs are proposed and have presented in our previous works [16, 20], and they can be respectively expressed as:

$$\Re_{11} = \tan\alpha_M/\tan\alpha_Q \tag{4}$$

https://doi.org/10.1017/S0263574725102762 Published online by Cambridge University Press

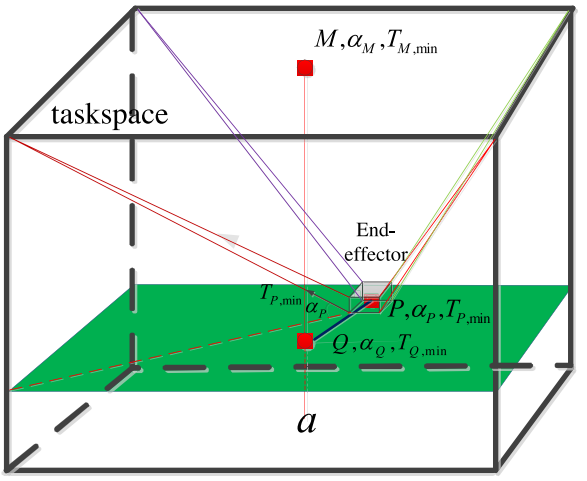


Figure 2. *Schematic diagram relating to PIFs and CTIFs.*

$$\Re_{21} = \tan\alpha_p / \tan\alpha_Q \tag{5}$$

where $\alpha = \arcsin\left(\dfrac{H-z}{\rho_{\min}}\right)$; $\rho_{\min}$ is the length of the cable having the minimum cable tension while the end-effector of the 8-6 CSPR is located at the present position P; and H is the height of the towers.

2.2. Cable tension influencing factor (CTIF)

This section presents statics equilibrium modeling for the 8-6 CSPR to propose the CTIFs. Referring to Fig. 1, the ith cable exerts a pure force at point B_i on the end-effector of the robot when tensions are maintained in the eight cables. And the tension can be written as $t_i\boldsymbol{d}_i$, where t_i is the nonnegative tension in the ith cable; meanwhile, the pure force generates a moment $({}^O\boldsymbol{R}_o\boldsymbol{b}_i) \times t_i\boldsymbol{d}_i$ at the reference point o. As a result, the wrench (force/moment pair) applied at o by the ith cable is $\begin{bmatrix} t_i\boldsymbol{d}_i \\ ({}^O\boldsymbol{R}_o\boldsymbol{b}_i) \times t_i\boldsymbol{d}_i \end{bmatrix}$. In this regard, the static equilibrium equation of the presented 8-6 CSPR could be expressed as:

$$\boldsymbol{JT} + \boldsymbol{W} = 0 \tag{6}$$

where $\boldsymbol{T} = [t_1 \sim t_2 \cdots t_8]^{\mathrm{T}}$ denotes the vector consisting of the eight cable tensions; $\boldsymbol{W}$ collects all other forces and torques acting on the end-effector of the 8-6 CSPR; and the pose-dependent matrix $J = [J_1\ J_2 \cdots J_8] = \begin{bmatrix} \boldsymbol{d}_1 & \boldsymbol{d}_2 & \cdots & \boldsymbol{d}_8 \\ ({}^O\boldsymbol{R}_o\boldsymbol{b}_1) \times \boldsymbol{d}_1 & ({}^O\boldsymbol{R}_o\boldsymbol{b}_2) \times \boldsymbol{d}_2 & \cdots & ({}^O\boldsymbol{R}_o\boldsymbol{b}_8) \times \boldsymbol{d}_8 \end{bmatrix}$ is the structure matrix of the presented 8-6 CSPR.

In practice, it is desirable to always have the cable tensions in a range between a lower and an upper limit. In detail, the lower limit is necessary to prevent cable slackness, which can lead to instability of robot, while the upper limit is imposed to avoid exceeding the tensile strength of the cables and the torque limits of the winch motors. Therefore, it is necessary to maintain the cable tensions within a safe and feasible range that ensures stability and performance of the 8-6 CSPR. As a result, one common issue for the presented 8-6 CSPR is that the cable tensions should not only satisfy the presented static equilibrium condition in Eq. (6) but also have a cable tension in a range between a lower limit $\boldsymbol{T}_{\mathrm{s,min}}$ and a higher limit $\boldsymbol{T}_{\mathrm{s,max}}$. As a result, the cable tensions satisfy the following relationship:

$$\boldsymbol{T}_{s,\min} \le \boldsymbol{T} \le \boldsymbol{T}_{s,\max} \tag{7}$$

where $\boldsymbol{T}_{\mathrm{s,min}}$ collects the lower bound of the cable tension to prevent cable looseness, while $\boldsymbol{T}_{\mathrm{s,max}}$ collects the upper bound of the cable tension to avoid cable breakage, which is generally set by the breaking loads of mechanical parts, the maximum actuator torques, or choice of material.

https://doi.org/10.1017/S0263574725102762 Published online by Cambridge University Press

As mentioned above, the investigated 8-6 CSPR is driven by eight cables, but the movement of the end-effector only includes translation and rotation in three directions. As a result, the 8-6 CSPR is a redundant cable-suspended parallel robot. Due to its redundancy in the 8-6 CSPRs, it can be seen form Eq. (6) that the number of cable actuators is more the degrees of freedom of the end-effector and, the structure matrix $\boldsymbol{J}$ is not square. As a result, there are infinite sets of tension distributions to generate a given wrench of the end-effector while the motion state of the robot's end-effector is known. Several studies and methods have presented in the literature to address this issue, such as optimizer approach with p-norm [27], closed-form solution [28], barycentric approach [29], and so on [30]. In order to obtain the optimal distributions of the cable tensions, minimization of the Euclidean norm of the relative cable tension vector, as a practical point of view, is presented to address the distributions of the eight cable tensions in this section. The basic idea of the presented method is to minimize the Euclidean norm of the difference between the actual cable tensions and the median feasible cable tensions. It should be noted that the optimized cable tensions must satisfy the static equilibrium Eq. (6) and remain within some specified upper and lower bounds $\boldsymbol{T}_{\text{s,min}}$ and $\boldsymbol{T}_{\text{s,max}}$ as shown in Eq. (7). In this section, the determination of the cable tensions for the 8-6 CSPRs can be formulated as follows:

$$\begin{aligned} &\text{Object } \min_{\boldsymbol{T}} \left\| \boldsymbol{T} - \overline{\boldsymbol{T}} \right\|_2 \\ &\text{subject to: } \boldsymbol{J}\boldsymbol{T} + \boldsymbol{W} = \boldsymbol{0} \\ &\text{and } \boldsymbol{T}_{s,\min} \le \boldsymbol{T} \le \boldsymbol{T}_{s,\max} \end{aligned}$$

where $\overline{\boldsymbol{T}} = \dfrac{\boldsymbol{T}_{s,\min} + \boldsymbol{T}_{s,\max}}{2}$ is vector of the medium feasible cable tensions.

It should be pointed out that the presented models and methods to obtain the cable tensions presented in this section are derived from ref. [27], and therefore, more information about investigating distributions of the cable tensions could be found in this paper. In addition, the minimum cable tension $T_{\min}$ while the end-effector of the 8-6 CSPRs locates at arbitrary pose within the workspace can be obtained based on the obtained unique solution to the cable tensions, and it can be expressed as:

$$T_{min} = min\ (\boldsymbol{T}) \tag{9}$$

where $T_{\min}$ is the smallest element in the cable tension $\boldsymbol{T}$.

Consequently, the cable with the minimum cable tension while the end-effector of the 8-6 CSPR is located at arbitrary pose within the workspace can be determined. In this regard, with reference to Fig. 2, two CTIFs have been proposed and used in our previous works [16, 20], and they can be respectively expressed as:

$$\Re_{12} = T_{P,\min}/T_{Q,\min} \tag{10}$$

$$\Re_{22} = T_{Q,\min}/T_{M,\min} \tag{11}$$

It should be pointed out that the presented two PIFs and two CTIFs, being a function of the end-effector's positions and cable tensions respectively, are all located in interval [0, 1], and in this regard, the proposed stability measure index for the 8-6 CSPRs with the two PIFs and two CTIFs can employ the interval [0, 1] to measure the stability of such robots.

2.3. The attitude influence function (AIF)

As already mentioned, the positions and attitudes of the end-effector as well as the cable tensions can affect the stability of the 8-6 CSPRs. However, the above studies only focused on analyzing the effects of the positions of the end-effector and cable tensions on the stability of the cable robots, and there is little research on the end-effector's attitudes on the stability of the 8-6 CSPRs. Due to modeling complexity of the coupling effects, researchers have not paid enough effort on investigating the effects of the end-effector's pose on the stability of the 8-6 CSPRs, especially the influence of the attitudes of the end-effector on the stability of the robot. In order to propose a systematic approach on the stability for the

https://doi.org/10.1017/S0263574725102762 Published online by Cambridge University Press

8-6 CSPRs, the effects of the end-effector's attitudes on the stability of the robots must be considered. Although the effects of the end-effector's positions and cable tensions have been researched, to the best of our knowledge, the most significant difference from existing research is that we are the first to investigate the effects of end-effector's attitudes on the stability of the 8-6 CSPRs. This section, as a result, introduces a contribution of this paper: the AIF of the stability for the 8-6 CSPRs is proposed. The idea for introducing the presented AIF is that the effects of the end-effector's attitudes on the stability of the 8-6 CSPRs can be considered and measured.

Apart from the above-mentioned factors in section 2.2, in addition, the end-effector's attitudes also have important effects on the stability of the 8-6 CSPRs. Therefore, this section is deliberately chosen to emphasize the effects of the attitudes on the stability of the robots. In order to quantify the effects, a function representing the effects of the attitudes of the end-effector on the stability for the robots, which is denoted by $f(\phi, \theta, \psi)$, is constructed at a later stage. To our knowledge, the presented paper is the first one to consider the effects of the end-effector's attitudes on the stability for the cable-driven parallel robots.

As mentioned above, the stability of the robot is indeed not solely determined by the orientation of the end-effector but is influenced by multiple factors, including the positions of the end-effector in space and the cable force distributions. As a matter of fact, the stability of the 8-6 CSPR while the end-effector is located at given position becomes weaker with the increase in the attitude angles of the end-effector, and this is because the center of gravity of the end-effector is closer to the tie line connecting the two hinge points between two adjacent cables. As a result, the orientation of the end-effector (0, 0, 0) is the most stable configuration for the 8-6 CSPR while the end-effector is located at a given position due to its symmetry, potential for even cable tensions, and farther distance between the center of gravity of the end-effector and tie line connecting the two hinge points between two adjacent cables. In this regard, the attitude angles (0, 0, 0) are seen as the most stable one while the center of gravity of the end-effector the robot is located at a given position. And furthermore, the stability of the 8-6 CSPRs at the present position with other attitudes is lower, and indeed, the stability is the weakest at the present position with the maximum attitude angles. Meanwhile, in order to employ the interval [0, 1] to assess the stability of the 8-6 CSPRs, the range of the AIF is the interval from 0 to 1.

Upon the analysis and discussion above, the proposed AIF is required to possess the following properties: (i) the range of the proposed AIF is the interval from 0 to 1 so as to employ the interval [0, 1] to measure the stability of the 8-6 CSPRs; (ii) the stability of the robots while the end-effector locates at the present position becomes weaker with the increase in the attitude angles; (iii) assume the present pose of the end-effector be $(x, y, z, \phi, \theta, \psi)$; moreover, two extreme cases should be discussed: on the one hand, the present pose with attitude angles (0, 0, 0) is the most stable one, and indeed, it is the stability measure not considering the effects of the attitudes on the stability of the 8-6 CSPRs; on the other hand, the present pose with maximum attitude angles $(\phi_{\max}, \theta_{\max}, \psi_{\max})$ is the weakest stability one, and therefore, let the stability of the 8-6 CSPRs at the attitudes be 0. It can also be noted that the stability of 8-6 CSPRs at other attitudes falls somewhere between the two extremes. In addition, the development of force-pose stability measures for 8-6 CSPRs is another novel contribution of this paper, as it will be explained further in the next section.

It is worth emphasizing that proposing an AIF representing the effects of the end-effector's attitudes on the stability of the 8-6 CSPRs for the 8-6 CSPRs is the main contribution of this work. And therefore, further insight into the problem of the determination of the proposed AIF $f(\phi, \theta, \psi)$ can be investigated from its geometric interpretation. In this regard, a schematic diagram relating to the AIF proposed in this paper is depicted in Fig. 3. Referring to Fig. 3, the perpendicular line between the mass center of the end-effector and the tie line connecting the two hinge points between two adjacent cables and the end-effector of the robot is noted by $\boldsymbol{n}_i$ when the three attitude angles of the end-effector equal to 0. It is worth emphasizing that the total tie lines and vectors $\boldsymbol{n}_i$ mainly depend on the connection mode and topological configuration of the eight cables and the end-effector of the robot. And furthermore, there are 12 connection lines for the presented 8-6 CSPR in this paper, which forms a space polygon. The gravity center line of the end-effector, generally speaking, is inside the proposed space polygon. It

https://doi.org/10.1017/S0263574725102762 Published online by Cambridge University Press

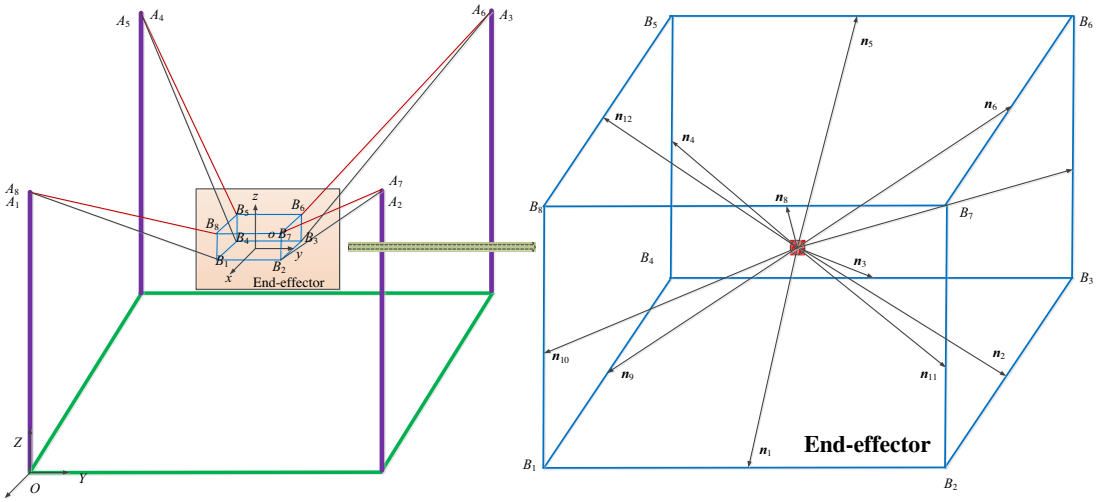


Figure 3. *Schematic diagram relating to the AIF.*

should be pointed that the 8-6 CSPRs is the most stable state with the three zero attitude angles when the end-effector is located at an arbitrary position within the workspace. In other words, the end-effector with the three zero attitude angles can be used as a reference to evaluate stability for the 8-6 CSPRs, while the robot possesses weaker stability when the end-effector has nonzero attitude angles. Note that the components along each coordinate axis of the vector $\boldsymbol{n}_i$ will change while the attitude angles of the end-effector vary. The gravity center line maybe goes beyond the space polygon as the increase of the attitude angles, which leads to instability of the 8-6 CSPRs. And furthermore, the shortest distance between the gravity center line of the end-effector and the space polygon indicates stability of the 8-6 CSPRs. From above, the components along each coordinate axis of the vector $\boldsymbol{n}_i$ can be employed to represent the effects of the end-effector attitude angles on the stability of the 8-6 CSPRs.

And as mentioned above, the presented AIF, which is primarily concerned with the question of which is the "shortest" distance between the gravity center line of the end-effector and the space polygon while the attitude angles of the end-effector of the 8-6 CSPR vary, is required to meet the properties above. Combined with the above discussion, in a particular manner,$f(\phi, \theta, \psi) =$

$$\min\left\{\begin{array}{l}\min\left(\dfrac{\left({}^{O}\boldsymbol{R}_{o}n_1\right)_x}{(n_1)_x}, \dfrac{\left({}^{O}\boldsymbol{R}_{o}n_1\right)_y}{(n_1)_y}, \dfrac{\left({}^{O}\boldsymbol{R}_{o}n_1\right)_z}{(n_1)_z}\right), \\ \cdots, \\ \min\left(\dfrac{\left({}^{O}\boldsymbol{R}_{o}n_i\right)_x}{(n_i)_x}, \dfrac{\left({}^{O}\boldsymbol{R}_{o}n_i\right)_y}{(n_i)_y}, \dfrac{\left({}^{O}\boldsymbol{R}_{o}n_i\right)_z}{(n_i)_z}\right), \\ \cdots, \\ \min\left(\dfrac{\left({}^{O}\boldsymbol{R}_{o}n_m\right)_x}{(n_m)_x}, \dfrac{\left({}^{O}\boldsymbol{R}_{o}n_m\right)_y}{(n_m)_y}, \dfrac{\left({}^{O}\boldsymbol{R}_{o}n_m\right)_z}{(n_m)_z}\right)\end{array}\right\}$$

meeting the three properties is deliberately chosen to represent the effects of the end-effector's attitudes on the stability of the 8-6 CSPR, while the proof of this is given below. $\dfrac{\left({}^{O}\boldsymbol{R}_{o}n_i\right)_x}{(n_i)_x}, \dfrac{\left({}^{O}\boldsymbol{R}_{o}n_i\right)_y}{(n_i)_y}, \dfrac{\left({}^{O}\boldsymbol{R}_{o}n_i\right)_z}{(n_i)_z}$ are ratios of the corresponding components along each coordinate axis of the vectors ${}^{O}\boldsymbol{R}_{o}n_i$ and $\boldsymbol{n}_i$ respectively, where the vector${}^{O}\boldsymbol{R}_{o}n_i$ is the distance between the gravity center line of the end-effector and the ith tie line with nonzero attitude angles. And it can be seen that $\min\left(\dfrac{\left({}^{O}\boldsymbol{R}_{o}n_i\right)_x}{(n_i)_x}, \dfrac{\left({}^{O}\boldsymbol{R}_{o}n_i\right)_y}{(n_i)_y}, \dfrac{\left({}^{O}\boldsymbol{R}_{o}n_i\right)_z}{(n_i)_z}\right)$ lays between 0 and 1, and therefore, the proposed AIF $f(\phi, \theta, \psi)$ is also between 0 and 1.

https://doi.org/10.1017/S0263574725102762 Published online by Cambridge University Press

3. The force-pose stability measure method

One of the primary concerns with the 8-6 CSPRs is the stability to the inevitable external disturbances. However, there, to our best knowledge, is no published technical paper about the force-pose stability measures for the 8-6 CSPRs. This section, based on the previous section, introduces another main contribution of this paper: force-pose stability measure method for the 8-6 CSPRs is proposed with the presented PIFs, CTIFs, and AIF. The proposed force-pose stability measure method of the 8-6 CSPRs addresses the problem of investigating their abilities to resist external disturbances. It should be pointed out that a closely related concept is the stiffness of the 8-6 CSPRs. Both are important for the performance of the 8-6 CSPR, but they address different aspects of the robot's behavior. On the one hand, the stiffness of the 8-6 CSPR is a measure of resistance to deformation when subjected to an external force, which mainly depends on the mechanical structure design, material properties, and connection methods of the robot. The stability of the robot, on the other hand, refers to the ability of the robot to maintain its equilibrium in the presence of external disturbances, which is affected by the end-effector's poses and cable tensions. And furthermore, the stiffness can contribute to stability of the robot, and in other word, high stiffness can enhance the stability of the 8-6 CSPR by reducing unwanted deformations that might otherwise cause instability. The majority of previous works dealing with the stability of the cable-driven parallel robots by considering the effects of the end-effector's positions, cable tensions and the stiffness on their stability for the cable-driven parallel robots [16–18]. However, these approaches have limitations, such as the effects of the end-effector's attitudes on the stability for the cable-driven parallel robots have apparently not been considered. Compared to refs. [16, 17, 31], the main improvement of the proposed force-pose stability measure method in this paper is to propose an AIF to measure the effects of end-effector's attitudes on the stability of the robots.

As has been mentioned above, the stability of the 8-6 CSPRs indicates the ability of robot to resist external interferences in the weakest constraint direction and to make the end-effector of the 8-6 CSPR be in equilibrium with external disturbances. In other words, the 8-6 CSPRs with high stability have a relatively high ability to resist external disturbances. Note that here the stability is associated with a particular pose where a family of cable tensions is required to make the end-effector be in equilibrium. Therefore, both the end-effector's poses and cable tensions have important effects on the stability of the 8-6 CSPRs. That is to say, the stability of the robot is pose-dependent and tension-dependent. Therefore, a systematic approach including combination of cable tensions and end-effector's poses on the stability of the 8-6 CSPRs is proposed in this paper. Particular emphasis was placed on the fact that the approach on the stability can employ the interval [0, 1] to measure the stability of the 8-6 CSPRs, leading to a stability workspace meeting the predetermined stability requirements.

Accordingly, the main contribution of this paper lies in the force-pose stability measure index (FPSI) for the 8-6 CSPRs based on the proposed CTIFs, PIFs, and AIF. Based on the aforementioned discussion, the proposed FPSI for the 8-6 CSPRs reads as:

$$S(\boldsymbol{X}, \boldsymbol{T}) = \prod_{l=1}^{2} (\mathrm{p}_{l1}\Re_{l1} + \mathrm{p}_{l2}\Re_{l2}) f(\phi, \theta, \psi) \tag{12}$$

where $\boldsymbol{X} = [x, y, z, \phi, \theta, \psi]$ is the end-effector's pose of the 8-6 CSPRs, $\boldsymbol{T}$ is the vector of eight cable tensions, and p_{i1} and p_{i2}, being between 0 and 1, are weight coefficients and meet the following conditions $\mathrm{p}_{l1}+\mathrm{p}_{l2} = 1$, $l = 1,2$. As mentioned before, both the two PIFs and the two CTIFs lay the interval from 0 to 1, and furthermore, the range of the proposed AIF lay the interval from 0 to 1. Therefore, the range of the FPSI $S(\boldsymbol{X}, \boldsymbol{T})$ for the 8-6 CSPRs lays the interval [0, 1], which implies that the proposed force-pose stability for the 8-6 CSPRs can employ the interval [0, 1] to measure the stability of the robots.

It should be pointed out that the proposed force-pose stability measure method for the 8-6 CSPR in this paper is different from that in the previous literature, in which the stability of the cable-driven parallel robots is regarded as the state of binary opposition between 0 and 1. In addition, it can be seen from that the proposed force-pose stability of the 8-6 CSPRs with given perturbations depends on the poses of the end-effector and the cable tensions. Meanwhile, numerous scholars have conducted

https://doi.org/10.1017/S0263574725102762 Published online by Cambridge University Press

extensive research on the workspace of the cable-driven parallel robots [32–34]. The force-pose stability analysis and measures are performed and, in this regard, a novel stability workspace for the 8-6 CSPRs is defined and generated with the proposed FPSI for this robot. For this reason, in this paper, we are interested in calculating the stability workspace of the 8-6 CSPRs for given end-effector's altitudes under the constraint that the force-pose stability of the robots does not exceed a given threshold based on numerical methods, in which the force-pose stability of the robot when the end-effector is located at arbitrarily pose of the workspace is determined with Eq. (12).

4. Force-pose stability sensitivity analysis method

It should be pointed out that there, to our best knowledge, is no published technical paper about the force-pose stability sensitivity analysis for the 8-6 CSPRs. Accordingly, the main contribution of this paper lies in proposing a force-pose stability sensitivity analysis method for the 8-6 CSPRs using the gray relational analysis method to reveal the sequence of the 14 influencing factors on the force-pose stability of the robot. As mentioned before, the force-pose stability measure method investigated in section 3 has demonstrated that the proposed PIF, CTIF, and AIF have significant effects on the stability for the presented 8-6 CSPRs. And in more detail, the presented PIF quantifies the influence of the end-effector's position on the stability of the robot, and further it captures how changes in the position of the end-effector affect the robot's stability. The presented CTIF assesses the impact of eight cable tensions on the robot's stability, and it reflects how variations in cable tensions influence the stability of the robot. The proposed AIF evaluates the influence of the attitudes of the end-effector on the robot's stability, and it helps in understanding how the attitudes of the end-effector contribute to the stability of the robot. We, in this section, focus on the sensitivity of the force-pose stability for the 8-6 CSPRs concerning the three positions and three attitudes of the end-effector, as well as eight cable tensions. The proposed FPSI for the 8-6 CSPR is affected by 14 factors in total, including 3 translational positions and 3 rotational attitudes of the end-effector, as well as 8 cable tensions, and therefore, the stability mechanism for the robot is extremely complex. In other word, the force-pose stability of the 8-6 CSPRs is a function of the aforementioned 14 influencing factors. And note that the importance of the proposed 14 influencing factors on the stability of the 8-6 CSPRs can be evaluated with the force-pose stability sensitivity analysis. The force-pose stability sensitivity analysis for the 8-6 CSPRs is to quantitatively investigate the influencing degrees of the 14 influencing factors on the stability of the 8-6 CSPRs. As a result, the gray relational degree, in the present paper, is employed to depict the correlation degree between the force-pose stability sequences and the 14 influencing factor sequences for the 8-6 CSPRs. The greater the sensitivity of the influencing factors on the force-pose stability of the 8-6 CSPRs, the more significant its influence on the robot's stability, and vice versa. Moreover, the main and secondary influencing factors,as well as the maximum and minimum influencing factors for the force-pose stability of the 8-6 CSPRs, can be accurately identified with the obtained gray correlation degrees. And therefore, through the force-pose stability sensitivity analysis, we can identify the influencing factors having great influence on the stability of the 8-6 CSPRs. As a result, a force-pose stability sensitivity analysis method for the 8-6 CSPRs is developed in this section using gray relational analysis. The most sensitive factor among the stability influencing factors can be identified and prioritized. In this section, the main steps of the proposed force-pose stability sensitivity analysis method are presented in the following section.

4.1. Determination of the force-pose stability and influencing factor sequences

According to the gray correlation theory [35–37], the correlation is determined by comparing the geometric similarity between the comparison sequences and the reference sequence. In more detail, the reference sequence reflects the system's behavioral characteristics, analogous to the dependent variable, while the comparative sequences composed of factors that influence the system's behavior, analogous to the independent variables. As a result, the numerical values of the proposed force-pose stability of the 8-6 CSPRs are set as the reference sequence, while a total of 14 influencing factors

https://doi.org/10.1017/S0263574725102762 Published online by Cambridge University Press

(the pose of the end-effector and the cable tensions) are set as the comparison sequences in this paper. And then, the reference and comparable sequences aredenoted as $\mathbf{\Theta}_0 = [\Theta_0(1), \Theta_0(2), \ldots, \Theta_0(k)]^{\mathrm{T}}$ and $\mathbf{\Theta}_i = [\Theta_i(1), \Theta_i(2), \ldots, \Theta_i(k)]^{\mathrm{T}}, i = 1,2, \ldots,14$, respectively. Moreover, it should be noted that k is the change number of the investigated 14 influencing factors and the force-pose stability for the 8-6 CSPRs in this paper. Therefore, the whole sequence matrix consisting of the two above sequences can be defined as follows:

$$\mathbf{\Theta} = \begin{bmatrix} \Theta_0(1) & \Theta_1(1) & \cdots & \Theta_{14}(1) \\ \Theta_0(2) & \Theta_1(2) & \cdots & \Theta_{14}(2) \\ \cdots & \cdots & \cdots & \cdots \\ \Theta_0(n) & \Theta_1(n) & \cdots & \Theta_{14}(n) \end{bmatrix} \tag{13}$$

4.2. Normalization of the sequence matrixes

The raw data of the presented force-pose stability reference sequence and the influencing factor comparison sequence, as a matter of fact, differ from the others in terms of their range and measure units, leading to the incomparable condition and even incorrect conclusion. Therefore, the main procedure first involves a normalization treatment on the initial data of the presented sequence matrixes. As a result, these sequences can be transformed with the following equation:

$$\Theta_i'(j) = \frac{\Theta_i(j) - \min\Theta_i(j)}{\max\Theta_i(j) - \min\Theta_i(j)}, (i = 0,1, \ldots,14; j = 1, 2, \ldots, n) \tag{14}$$

4.3. Gray correlation coefficient

The presented sequence matrixes are standardized, and in this regard, the absolute difference between the force-pose stability reference sequence and the 14 influencing factor comparison sequences, denoted by $\Delta_{0i} = |\Theta_0(j) - \Theta_i(j)|, i = 0, 1, \ldots, 14$, can be computed. And then, the maximum difference is denoted by $\Delta_{\max} = \max_{1\le i\le 14} \max_{1\le j\le n} |\Theta_0(j) - \Theta_i(j)|$ and the minimum difference is denoted by $\Delta_{\min} = \min_{1\le i\le 14} \min_{1\le j\le n} |\Theta_0(j) - \Theta_i(j)|$. Thereupon, the gray relation coefficients can be computed with the following formula:

$$r_{ij}(j) = \frac{\Delta_{\min} + \xi\Delta_{\max}}{\Delta_{0i}(j) + \xi\Delta_{\max}} \tag{15}$$

where ξ is the distinguishing coefficient.

4.4. Gray correlation force-pose stability sensitivity analysis index

The correlation between the proposed force-pose stability reference sequence and influencing factor compared sequences for the 8-6 CSPRs can be represented by gray relational degree. As a result, if a certain influencing factor in compared sequence is far more critical than other influencing factors to the force-pose stability for the 8-6 CSPRs, the gray correlation degree of this influencing factor will be higher than others. In that case, the gray correlation degree can be employed to measure the influence degree of the positions and attitudes of the end-effector, as well as the cable tensions on the force-pose stability of the 8-6 CSPRs. It is noteworthy that the main influencing factors and secondary influencing factors, and the maximum and minimum influencing factors for the force-pose stability of the 8-6 CSPRs, in more detail, can be obtained through the correlation degrees of the 14 influencing factors. To sum up, a gray correlation sensitivity analysis method for the force-pose stability of the 8-6 CSPRs is proposed and measured with the gray correlation degree, and the proposed force-pose stability sensitivity analysis index for the 8-6 CSPRs reads as:

$$R_i = \frac{1}{n}\sum_{j=1}^{n} r_{ij}(j) \tag{16}$$

https://doi.org/10.1017/S0263574725102762 Published online by Cambridge University Press

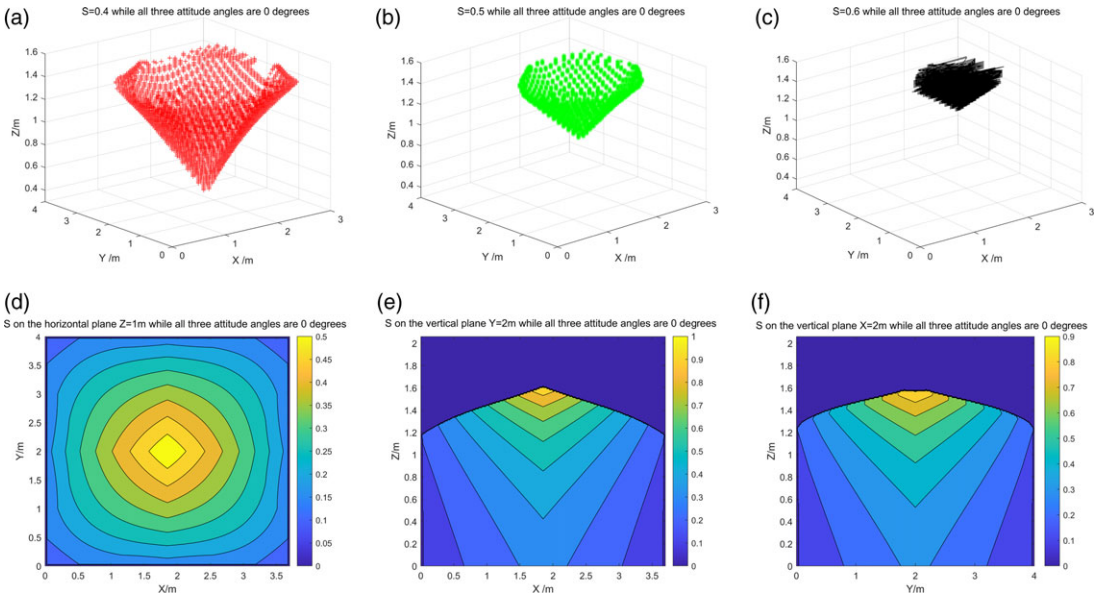


Figure 4. *The distributions of FPSI within specific regions of the workspace with* $(\phi, \theta, \psi) = (0°, 0°, 0°)$.

5. Simulation examples and results

In this section, the developed force-pose stability measure method and the force-pose stability sensitivity analysis method are implemented on a typical spatial CSPR driven by eight cables through simulations. The selected 8-6 CSPR is shown in Fig. 1, in which the base is a cube of 3.7 × 4.0 × 2.3 (m), and the moving platform is a cube with the dimension of 0.1 × 0.1 × 0.1 (m). Referring to Fig. 1, the fixed reference frame for the 8-6 CSPR is located at the bottom of the first column. And therefore, the position vectors that the cables enter the pulleys are $\boldsymbol{A}_1 = [0, 0, 2.3]^{\mathrm{T}}$ m, $\boldsymbol{A}_2 = [0, 4.0, 2.3]^{\mathrm{T}}$ m, $\boldsymbol{A}_3 = [-3.7, 4.0, 2.3]^{\mathrm{T}}$ m, $\boldsymbol{A}_4 = [-3.7, 0, 2.3]^{\mathrm{T}}$ m, $\boldsymbol{A}_5 = [-3.7, 0, 2.3]^{\mathrm{T}}$ m, $\boldsymbol{A}_6 = [-3.7, 4.0, 2.3]^{\mathrm{T}}$ m, $\boldsymbol{A}_7 = [0, 4.0, 2.3]^{\mathrm{T}}$ m, and $\boldsymbol{A}_8 = [0, 0, 2.3]^{\mathrm{T}}$ m. In addition, the local frame is located at the gravity center of the end-effector. The pose of the end-effector is denoted by $(x,y,z,\phi, \theta, \psi)^{\mathrm{T}}$, where the pose of the end-effector is $(x,y,z,0, 0, 0)^{\mathrm{T}}$. As a result, the vectors from the gravity center of end-effector to the cable attachment points are $b_1 = [-0.1, 0.1, -0.1]^{\mathrm{T}}$ m, $b_2 = [0.1, 0.1, -0.1]^{\mathrm{T}}$ m, $b_3 = [0.1, -0.1, -0.1]^{\mathrm{T}}$ m, $b_4 = [-0.1, -0.1, -0.1]^{\mathrm{T}}$ m, $b_5 = [-0.1, -0.1, 0.1]^{\mathrm{T}}$ m, $b_6 = [0.1, -0.1, 0.1]^{\mathrm{T}}$ m, $b_7 = [0.1, 0.1, 0.1]^{\mathrm{T}}$ m, and $b_8 = [-0.1, 0.1, 0.1]^{\mathrm{T}}$ m. It is noteworthy that the weight of the end-effector is 10 kg and, the lower limit $\boldsymbol{T}_{\mathrm{s,min}}$ and a higher limit $\boldsymbol{T}_{\mathrm{s,max}}$ of the employed cables are assumed to be 1 and 100 N, respectively.

This section aims at investigating the proposed FPSI within specific regions of the workspace and comparing the proposed stability workspace for the 8-6 CSPR. And the distributions of the proposed FPSI within specific regions of the workspace and the three attitude angles $(\phi, \theta, \psi) = (0, 0, 0)$ are shown in Fig. 4, and the AIF is equal to 1 as the three attitude angles $(\phi, \theta, \psi) = (0, 0, 0)$. This presented stability workspace of the 8-6 CSPR is calculated and recorded by discretizing and exhaustively searching the taskspace of the robot through discrete calculation, and the space surfaces surrounded by $S = 0.4$, $S = 0.5$, and $S = 0.6$ are shown in Fig. 4(a)–(c). And furthermore, from the above results from the three figures, we can see that with the increase of the predetermined stability conditions, the achievable workspace of the robot's end-effector decreases. On the whole, it should be pointed out that the minimum stability over the presented stability workspace for the robot is 0.4 with the three attitude angles $(\phi, \theta, \psi) = (0, 0, 0)$. In fact, the presented stability workspace of the 8-6 CSPR is within the constant orientation workspace of the robot when the three attitude angles of the end-effector are fixed as $(\phi, \theta, \psi) = (0, 0, 0)$. In more detail, the presented stability workspace of the robot is calculated and

https://doi.org/10.1017/S0263574725102762 Published online by Cambridge University Press

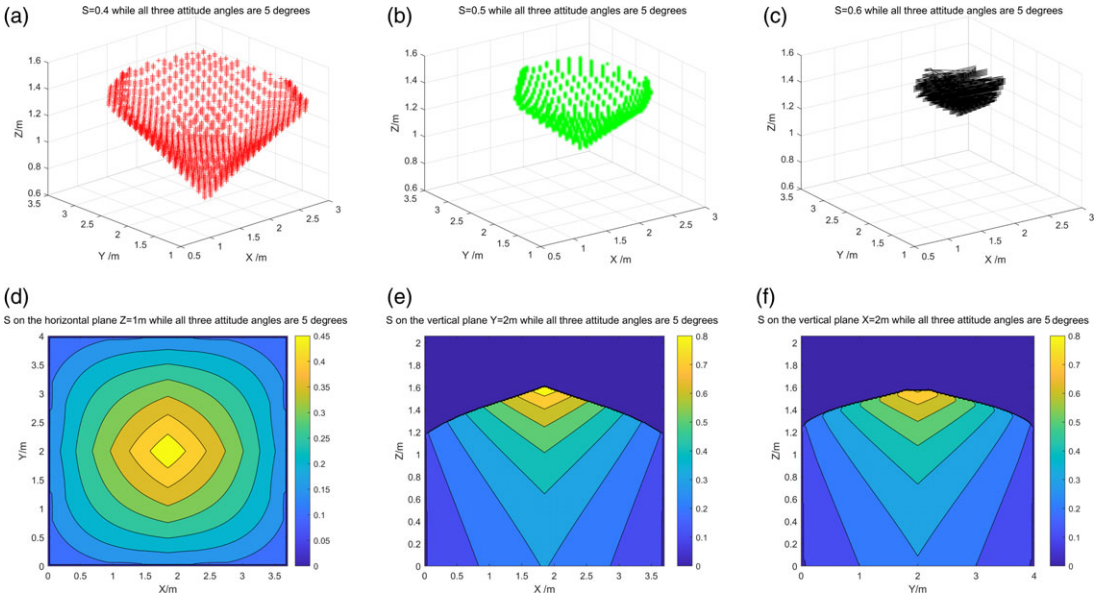


Figure 5. *The distributions of FPSI within specific regions of the workspace with* $(\phi, \theta, \psi) = (5°, 5°, 5°)$.

recorded by discretizing and exhaustively searching the taskspace through 322506 times discrete calculation, and 24,954 positions of end-effector are located within the presented space surface as shown in Fig. 4(a). To visually display the proposed FPSI and the stability workspace, the distributions of FPSI within in some specific planes of the workspace are generated and depicted with the three attitude angles $(\phi, \theta, \psi) = (0, 0, 0)$, as shown in Fig. 4(d)–(f). It is can be seen that the 8-6 CSPR hold the bigger FPSI when the end-effector locates at the top and the center of the workspace than others, and it is worth emphasizing that there is a good agreement between the obtained results with the conclusion of ref. [16]. That is to say, the 8-6 CSPR has stronger stability as the end-effector operates in these areas of the taskspace.

Moreover, the distributions of the proposed FPSI within specific regions of the workspace and the three attitude angles of the end-effector $(\phi, \theta, \psi) = (5, 5, 5)$ and $(\phi, \theta, \psi) = (10, 10, 10)$ are depicted in Figs. 5 and 6. Comparing Figs. 4, 5, and 6, it can be seen that the volume of the obtained stability workspace, as the attitude angle of the end-effector changes from 0 to 5 degree and from 0 to 10 degree, has been a sharp decrease. Therefore, it can be concluded that the end-effector's attitude angle has an important influence on the stability of the robot.

From above, through the simulation results and comparative analysis, it is found that the stability measure approach with a force-pose property and the presented stability workspace for the 8-6 CSPRs is reasonable and effective. It is possible to examine and determine how the geometry of the proposed stability workspace is affected by the varying of different end-effector's poses and cable tensions, similar to what was done for point-mass CDPR in ref. [16]. Moreover, this stability measure approach presented in this paper can readily be applied to the point-mass CDPR as the AIF is set to 1. And as mentioned in Section 3, the proposed force-pose stability measure method employs the quantifiable numbers [0, 1] to measure the stability of the 8-6 CSPRs, which is different from the traditional methods that simply regard the stability of cable-driven parallel robots as two states: a stable state and a nonstable one. As a matter of fact, it is very important and meaningful to identify a specific stability threshold where the 8-6 CSPRs become unstable. However, the specific stability threshold of the proposed force-pose stability measure method for the 8-6 CSPRs is closely related to the configuration, external disturbances, and working conditions of the robots. For this reason, our future work could involve investigating and identifying a specific stability threshold for the proposed force-pose stability measure method to distinguish whether the robot is stable or not.

https://doi.org/10.1017/S0263574725102762 Published online by Cambridge University Press

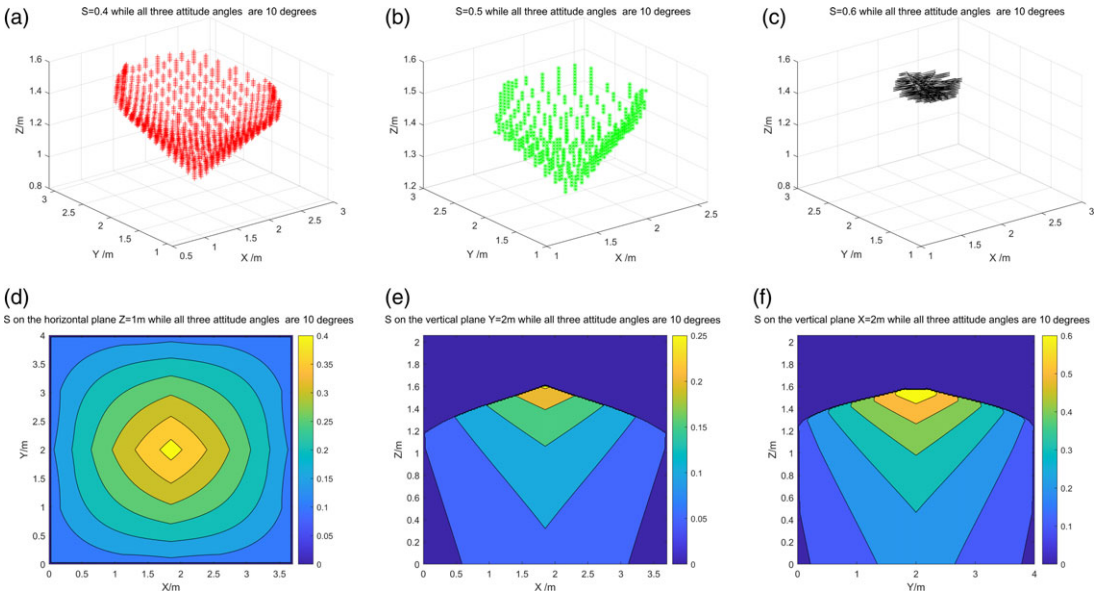


Figure 6. *The distributions of FPSI within specific regions of the workspace with* $(\phi, \theta, \psi) = (10°, 10°, 10°)$.

In the following, it is interesting to investigate the importance of the 14 influencing factors on the stability of the 8-6 CSPRs with the proposed force-pose stability sensitivity analysis method for the 8-6 CSPRs based on the gray relational analysis. The gray relational analysis method has significant advantages in the stability sensitivity analysis of the 8-6 CSPRs, mainly reflected in the following aspects: less data required, elimination of dimensional influence, identification of key influencing factors, and so on [20–22]. It is particularly important that the gray relational analysis method does not require a large amount of sample data and can effectively conduct analysis based on a limited amount of data. As a result, a spiral trajectory (Fig. 7) for the end-effector of the 8-6 CSPR is selected to obtain the original data of the force-pose stability and its 14 influencing factors for the 8-6 CSPR. It should be noted that this is a dynamic trajectory defined as a sequence of the poses for the end-effector of the 8-6 CSPR, and the used spiral trajectory is within the stability workspace of the robot. Furthermore, when controlling the end-effector of the 8-6 CSPR to move the given spiral trajectory, the length of the eight cables can be obtained with the kinematic equations of robots. Nevertheless, the proposed force-pose stability of the 8-6 CSPRs, in this paper, is closely related to the end-effector's poses and the eight cable tensions, but not to the length of the eight cables. As a result, the response values of the cable tensions of the eight cables and the poses of the end-effector are calculated along with the force-pose stability for the 8-6 CSPR, and the obtained results are shown in Table I.

As shown in Table I, the original data of the force-pose stability and the 14 influencing factors are obtained while the end-effector of the 8-6 CSPR is located on the selected spiral trajectory. And note that the eight cable tensions (T_1–T_8) in Table I are obtained considering the dynamic characteristics of the end-effector on the selected spiral trajectory. It can be also seen from Table I that the 14 influencing factors and the proposed stability have their own quite different dimensions and numerical values. Therefore, the 14 influencing factor sequences and the force-pose stability reference sequence should be non-dimensionalized employing Eq. (14) to compute gray correlation grades, and the obtained results of dimensionless processing of the original data are shown in Table II. Based on the deviation sequence matrix of each influencing factor sequence and the obtained force-pose stability reference sequence for the 8-6 CSPR, the correlation coefficient matrix r can be obtained with the following formula (17):

https://doi.org/10.1017/S0263574725102762 Published online by Cambridge University Press

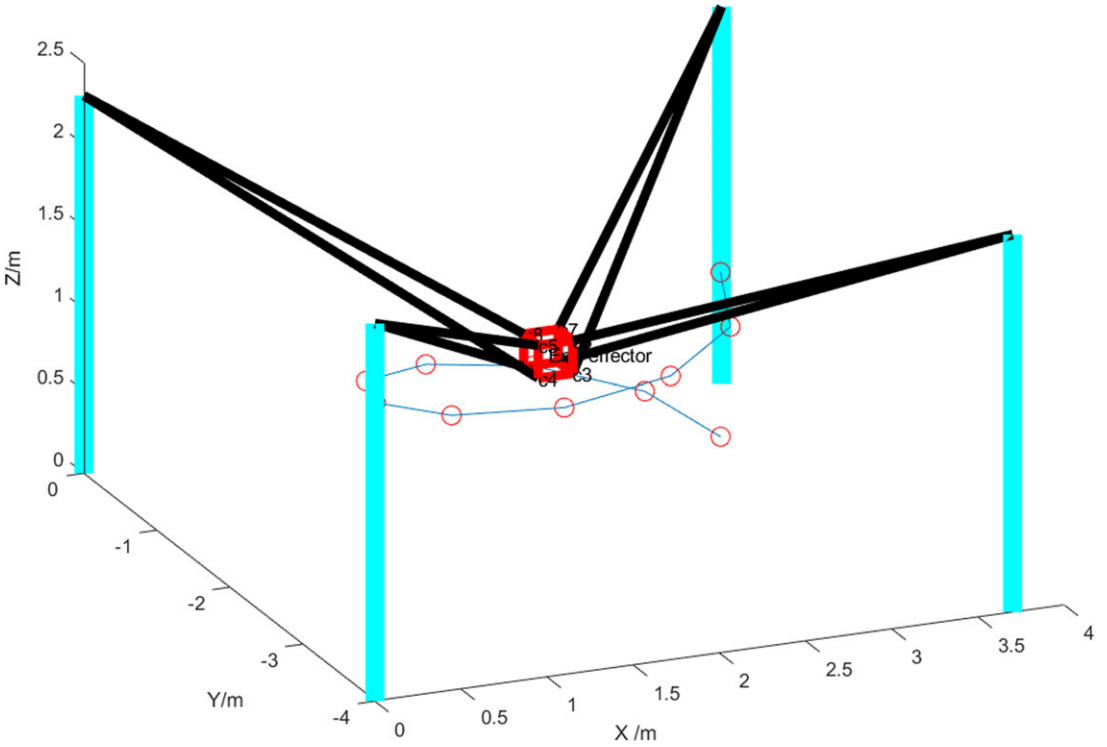


Figure 7. *The selected spiral trajectory for the end-effector of the 8-6 CSPR.*

$$r = \begin{bmatrix} 0.6803 & 0.7696 & 0.9012 & 0.5949 & 0.5949 & 0.5949 & 0.5949 & 0.8658 & 0.5935 & 0.6092 & 0.6281 & 0.6060 & 0.7252 & 0.4312 \\ 1 & 0.7232 & 1 & 0.3333 & 0.3333 & 0.3333 & 0.6432 & 1 & 0.8173 & 0.6391 & 0.3924 & 1 & 1 & 0.3333 \\ 0.4330 & 0.8788 & 0.8788 & 0.7355 & 0.9808 & 0.4432 & 0.4612 & 0.5981 & 0.4644 & 0.6564 & 0.3494 & 0.7903 & 0.8327 & 0.4913 \\ 0.8383 & 0.4895 & 0.6795 & 0.8894 & 0.5760 & 0.5443 & 0.4895 & 0.8406 & 0.6128 & 0.5110 & 0.5993 & 0.8487 & 0.8988 & 0.6499 \\ 0.4251 & 0.9134 & 0.9134 & 0.5236 & 0.9398 & 0.3442 & 0.7356 & 0.9904 & 0.3817 & 0.5396 & 0.9134 & 0.7686 & 0.4024 & 0.7335 \\ 0.6422 & 0.8286 & 0.9269 & 0.5101 & 0.3580 & 0.6277 & 0.8337 & 0.8286 & 0.4896 & 0.4527 & 0.7454 & 0.8634 & 0.5036 & 0.4639 \\ 0.7336 & 0.8406 & 0.9124 & 0.3777 & 0.3598 & 0.3823 & 0.8830 & 0.9653 & 0.3558 & 0.4548 & 0.6489 & 0.8619 & 0.6156 & 0.3868 \\ 0.7460 & 0.4836 & 0.6285 & 0.5593 & 0.7889 & 0.7367 & 0.5561 & 0.7483 & 0.7720 & 0.7874 & 0.4263 & 0.9154 & 0.9051 & 0.5726 \\ 0.5524 & 0.8406 & 0.9553 & 0.7618 & 0.5827 & 0.8223 & 0.9808 & 0.9827 & 0.5957 & 0.6234 & 0.4913 & 0.5524 & 0.5524 & 0.4914 \\ 0.8257 & 0.7237 & 0.6364 & 0.3333 & 0.7978 & 0.4177 & 0.7958 & 0.9807 & 0.3333 & 0.3333 & 0.4133 & 0.8129 & 0.7073 & 0.4155 \end{bmatrix} \quad (17)$$

And then, according to Eq. (16), the gray correlation degree between the 14 influencing factors and the proposed force-pose stability for the 8-6 CSPRs are calculated, and the correlation degree between the force-pose stability and each influencing factor mentioned above for the 8-6 CSPRs is shown in Table III. According to the calculation results in Table III, the results of gray correlation are calculated as follows: correlation degree of x-direction displacement: $R_x = 0.688$; correlation degree of y-direction displacement: $R_y = 0.794$; correlation degree of z-direction displacement: $R_z = 0.843$; correlation degree of the attitude angle of rotation around x axis: $R_\phi = 0.562$; correlation degree of the attitude angle of rotation around y axis: $R_\theta = 0.631$; correlation degree of the attitude angle of rotation around z axis: $R_\psi = 0.525$; correlation degree of cable tension 1: $R_{T1} = 0.697$; correlation degree of cable tension 2: $R_{T2} = 0.880$; correlation degree of cable tension 3: $R_{T3} = 0.542$; correlation degree of cable tension 4: $R_{T4} = 0.561$; correlation degree of cable tension 5: $R_{T5} = 0.561$; correlation degree of cable tension 6: $R_{T6} = 0.802$; correlation degree of cable tension 7: $R_{T7} = 0.714$; and correlation degree of cable tension 8: $R_{T8} = 0.497$. One can see from the obtained data that the cable tension T_2 has the highest correlation with the proposed force-pose stability of the 8-6 CSPR, which is 0.880, whereas the cable tension T_8 has the least correlation to the force-pose stability of the robot, being only 0.497. It should be pointed out that the 14 influencing factors on the force-pose stability of the 8-6 CSPR can be divided into the

https://doi.org/10.1017/S0263574725102762 Published online by Cambridge University Press

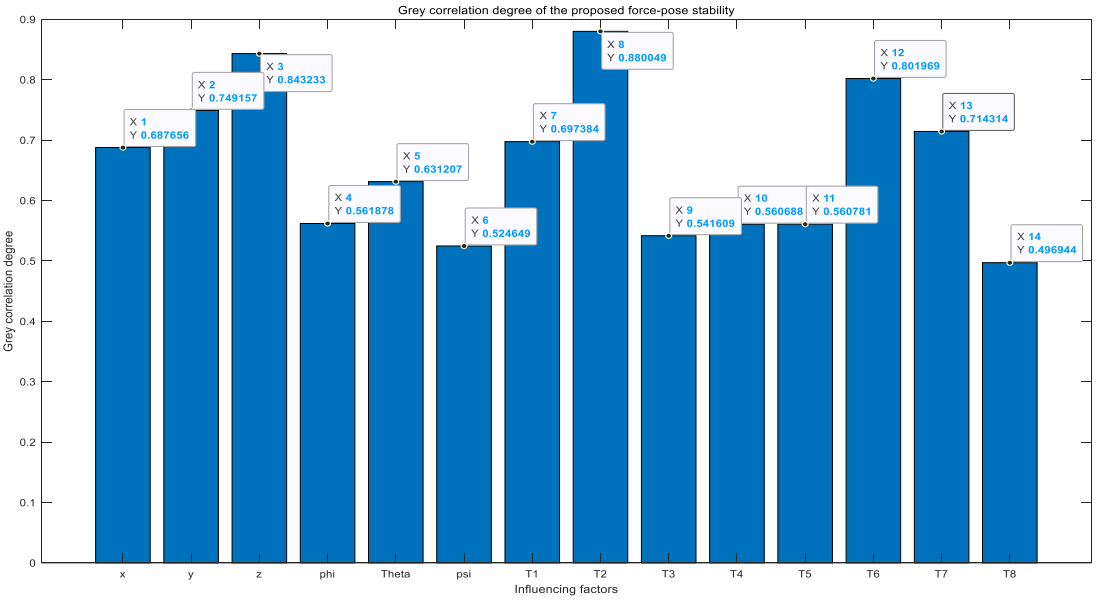


Figure 8. *Gray correlation degree of the proposed force-pose stability and influencing factors with* $\xi = 0.5$.

three PIFs, three attitude influencing factors, and eight cable tension factors. It is important to note that, on the whole, the mean value of the gray correlation degree of the end-effector's position on the force-pose stability sensitivity of the robot is 0.775; meanwhile, the mean value of the gray correlation degree of the end-effector's attitude on the force-pose stability sensitivity of the robot is 0.573; moreover, the mean value of the gray correlation degree of the cable tension on the force-pose stability sensitivity of the robot is 0.657. Accordingly, it can be inferred that the positions of the end-effector have more significant influences on the force-pose stability of the 8-6 CSPR than the attitudes of the end-effector and the cable tensions. In this regard, the force-pose stability of the 8-6 CSPR is more sensitive to the positions of the end-effector, followed by the cable tensions and the attitudes of the end-effector. As a result, in order to reduce the influence of the end-effector's positions on the stability of the 8-6 CSPR, it is essential to prioritize the precise control of the end-effector's positions.

One can see from Fig. 8 that the gray correlation degrees of the 14 influencing factors on the force-pose stability of the 8-6 CSPR with the distinguishing coefficient $\xi = 0.5$ are shown in the descending order as follows: cable tension T_2 > z-direction displacement of the end-effector > cable tension T_6 > y-direction displacement > cable tension T_7 > x-direction displacement of the end-effector > attitude angle of the end-effector about y-axis θ > attitude angle of the end-effector about x-axis ϕ > cable tension T_5 > cable tension T_4 > cable tension T_3 > attitude angle of the end-effector about z-axis ψ > cable tension T_8. Moreover, the gray correlation degrees of the 14 influencing factors on the force-pose stability of 8-6 CSPR with the distinguishing coefficient $\xi = 0.6$ are presented in Fig. 9. It can be seen from the two figures that the sequence of gray correlation degrees of the 14 influencing factors on the force-pose stability of the 8-6 CSPR, with regard to different distinguishing coefficient, consistents with each other. And furthermore, it can be seen from the figure that the obtained gray correlation degrees of the PIFs, attitude influencing factors, and the CTIFs, apart from the cable tension T_8, are basically greater than 0.5, indicating that the presented 14 factors have an important influence on the force-pose stability of the 8-6 CSPR.

To sum up, this presented work aimed to investigate the force-pose stability for the 8-6 CSPRs in two key areas: force-pose stability measures and stability sensitivity analysis; moreover, the proposed models, methods, and obtained results for the 8-6 CSPRs are verified through simulations in this paper. Nevertheless, it is also important that an experimental validation on the physical prototype of the 8-6

https://doi.org/10.1017/S0263574725102762 Published online by Cambridge University Press

https://doi.org/10.1017/S0263574725102762 Published online by Cambridge University Press

Table I. *Original data of the force-pose stability and influencing factors.*

Nos.	S	x**(m)**	y**(m)**	z**(m)**	ϕ**(rad)**	θ**(rad)**	ψ**(rad)**	T_1**(N)**	T_2**(N)**	T_3**(N)**	T_4**(N)**	T_5**(N)**	T_6**(N)**	T_7**(N)**	T_8**(N)**
1	0.332	1.041	1.412	0.900	0	0	0	19.328	25.3928	29.856	29.947	32.976	4.664	7.307	44.090
2	0.485	2.659	2.587	1.400	0	0	0	37.847	43.300	32.059	30.772	16.259	58.065	44.547	14.358
3	0.269	2.159	1.049	0.700	0.052	0.087	0.122	36.066	24.991	29.456	25.102	47.770	14.762	8.114	31.804
4	0.364	1.541	2.951	1.200	0.087	0.122	0.157	44.953	30.169	24.270	20.257	40.145	34.613	19.201	20.576
5	0.264	2.159	1.049	0.700	0.105	0.017	0.175	25.148	13.840	31.728	27.203	7.063	14.563	35.328	21.170
6	0.277	1.541	1.049	0.800	0.122	1.105	0.070	19.424	12.531	29.231	30.632	18.226	13.730	26.837	34.613
7	0.463	2.159	2.951	1.300	0.017	0.017	0.017	40.826	39.830	22.526	24.737	32.896	48.578	26.695	17.702
8	0.317	1.041	2.589	1.100	0.140	0.157	0.017	36.624	26.193	23.902	26.277	45.685	16.285	10.483	33.658
9	0.347	0.850	2.000	1.000	0.052	0.052	0.052	29.460	25.269	30.517	30.620	44.630	3.828	0.683	41.788
10	0.253	1.041	1.412	0.900	0.209	0.140	0.122	22.616	12.834	33.259	34.910	35.959	10.069	9.760	35.267

https://doi.org/10.1017/S0263574725102762 Published online by Cambridge University Press

Table II. *Results of dimensionless processing of raw data.*

Nos.	S	x**(m)**	y**(m)**	z**(m)**	ϕ**(rad)**	θ**(rad)**	ψ**(rad)**	T_1**(N)**	T_2**(N)**	T_3**(N)**	T_4**(N)**	T_5**(N)**	T_6**(N)**	T_7**(N)**	T_8**(N)**
1	0.341	0.106	0.191	0.286	0	0	0	0	0.418	0.683	0.661	0.637	0.015	0.151	1
2	1	1	0.809	1	0	0	0	0.723	1	0.888	0.718	0.226	1	1	0
3	0.069	0.724	0	0	0.249	0.079	0.697	0.653	0.405	0.646	0.331	1	0.202	0.169	0.587
4	0.478	0.382	1	0.714	0.417	0.110	0.897	1	0.573	0.162	0	0.813	0.568	0.442	0.209
5	0.047	0.724	0	0	0.502	0.015	1	0.227	0.043	0.857	0.474	0	0.198	0.790	0.229
6	0.103	0.382	0	0.143	0.584	1	0.400	0.004	0	0.625	0.708	0.274	0.183	0.596	0.681
7	0.905	0.724	1	0.857	0.081	0.015	0.097	0.838	0.887	0	0.306	0.635	0.825	0.593	0.112
8	0.275	0.106	0.810	0.571	0.670	0.142	0.097	0.675	0.444	0.128	0.411	0.949	0.230	0.223	0.649
9	0.405	0	0.500	0.429	0.249	0.047	0.297	0.395	0.414	0.745	0.707	0.993	0	0	0.923
10	0	0.10	0.191	0.286	1	0.127	0.697	0.128	0.010	1	1	0.710	0.115	0.207	0.703

Table III. *Sequence of gray correlation degrees of the 14 influencing factors for the 8-6 CSPR.*

Influencing factors	**Gray correlation degree**	**Ranking**
Position of the end-effector in x-axis	0.688	7
Position of the end-effector in y-axis	0.749	4
Position of the end-effector in z-axis	0.843	2
Attitude angle of the end-effector about x-axis (ϕ)	0.562	9
Attitude angle of the end-effector about y-axis (θ)	0.631	8
Attitude angle of the end-effector about z-axis (ψ)	0.525	13
Tension of cable 1 (T_1)	0.697	6
Tension of cable 2 (T_2)	0.880	1
Tension of cable 3 (T_3)	0.542	12
Tension of cable 4 (T_4)	0.561	11
Tension of cable 5 (T_5)	0.561	10
Tension of cable 6 (T_6)	0.802	3
Tension of cable 7 (T_7)	0.714	5
Tension of cable 8 (T_8)	0.497	14

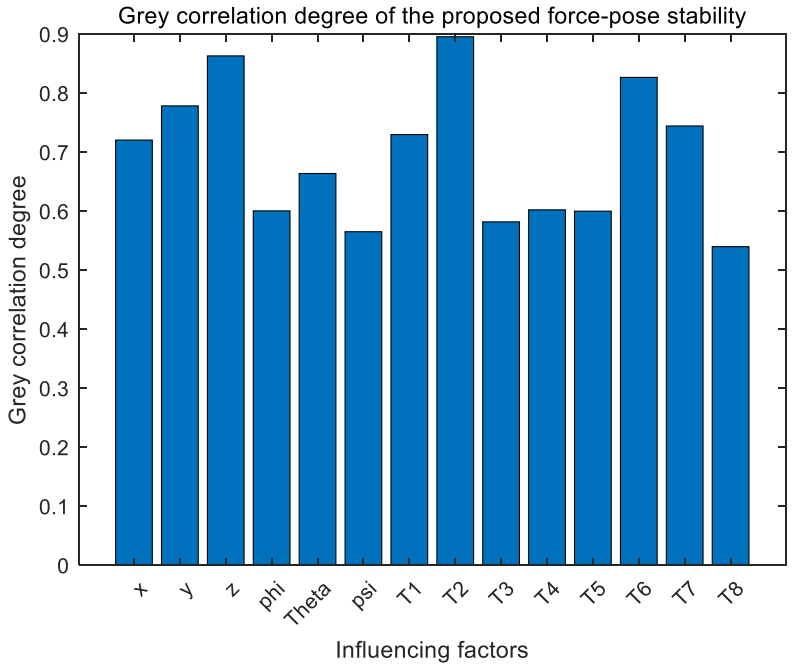


Figure 9. *Gray correlation degree of the proposed force-pose stability and influencing factors with* $\xi = 0.6$.

CSPR is the most convincing way to demonstrate the practical value of the proposed models, methods, and the obtained results in this paper. Thereupon, we will build an experimental platform for a six-DOF cable-driven parallel robot with eight cables at our laboratory, and each cable will equip with a calibrated load cell and the end-effector's pose is tracked by a laser tracker.

6. Conclusions and future works

The main contribution of the investigation is extending an early developed force-position stability measure method for a cable-driven parallel robot for aerial panoramic photographing by proposing an AIF

https://doi.org/10.1017/S0263574725102762 Published online by Cambridge University Press

for the 8-6 CSPRs. The main motivation of employing the AIF for 8-6 CSPRs is that the end-effector's attitudes have important effects on the stability of the robot. In summary, this presented work aimed to investigate the force-pose stability for the 8-6 CSPRs in two key areas: force-pose stability measures and stability sensitivity analysis. The main contributions of this work include the following:

(i) A force-pose stability measure method for the 8-6 CSPRs is presented in this paper, based on the proposed two PIFs, two CTIFs, and an AIF. The force-pose stability measures for the 8-6 CSPRs, which are pose-dependent and tension-dependent, can employ the interval [0, 1] to solve the stability of the robots. And furthermore, the proposed force-pose stability measure method is verified by simulation, and the results show the importance of taking into consideration the effects of the end-effector's attitudes on the stability for the 8-6 CSPRs.

(ii) The force-pose stability of the 8-6 CSPRs is influenced by 14 factors, such as the cable tensions, the positions, and the attitudes of the end-effector, and further the 14 influencing factors have different sensitivity to the force-pose stability of the robot. As a result, the sensitivity analysis model for the force-pose stability of the 8-6 CSPRs is developed with the gray relational analysis method to reveal the sequence of the 14 influencing factors on the force-pose stability of the robot. Through the analysis of the force-pose stability sensitivity for the 8-6 CSPRs, the key elements that affect the stability of the robots are identified.

(iii) The proposed force-pose stability measure method and gray relational sensitivity analysis method to the force-pose stability for the 8-6 CSPRs are performed by simulations. With regard to the presented 14 influencing factors on the force-pose stability of the 8-6 CSPRs, the importance has following sequence: cable tension T_2 > z-direction displacement of the end-effector > cable tension T_6 > y-direction displacement > cable tension T_7 > x-direction displacement of the end-effector > attitude angle of the end-effector about y-axis θ > attitude angle of the end-effector about x-axis ϕ > cable tension T_5 > cable tension T_4 > cable tension T_3 > attitude angle of the end-effector about z-axis ψ > cable tension T_8. Moreover, on the whole, the mean value of the gray correlation degree of the end-effector's positions, the end-effector's attitudes, and the cable tensions on the force-pose stability sensitivity of the 8-6 CSPRs is 0.775, 0.573, and 0.657, respectively. Therefore, the positions of the end-effector have more significant influences on the force-pose stability of the 8-6 CSPR than the attitudes of the end-effector and the cable tensions.

From above, the presented work puts forward a comprehensive methodology for investigating the stability and stability sensitivity for the 8-6 CSPRs while considering the effects of the end-effector's poses and the cable tensions on the stability of the robots. It should be noted that the findings obtained from this paper can be extended to other configurations while considering the effects of the attitudes of the end-effector on the stability of the robots. Meanwhile, the stiffness of the 8-6 CSPRs is another critical property that significantly influences the performance and stability of these robots. As a consequence, future work could involve integrating the stiffness analysis into the stability and stability sensitivity to offer more holistic insights into optimizing the performance of the robots. And furthermore, it is central to the presented investigation to measure the proposed force-pose stability for the 8-6 CSPRs by experiments. Therefore, future work will concentrate on the experimental measurement and verification of the proposed force-pose stability for the 8-6 CSPRs with pose drift ratio and tension-induced stiffness index that depend simultaneously on pose deviation and tension variation.

Author contributions. Peng Liu and Xuechao Duan conceived and designed the study. Zhufeng Shao provides special guidance in the theoretical part of this paper. Jing Xia participated in the translation and proofreading of the paper. Peng Liu wrote the article. All authors have read and agreed to the published version of the manuscript.

Financial support. The authors gratefully acknowledge the financial support of National Science and Technology Major Project on Clean and Efficient Utilization of Coal for Supporting Energy Transition under Grant No. 2025ZD1700600, Shaanxi Province Natural Science Basic Research Program Project under Grant No. 2024JC-YBMS-324, Education Department of Shaanxi

https://doi.org/10.1017/S0263574725102762 Published online by Cambridge University Press

Provincial Government Service Local Special Project under Grant No. 23JC053, and Bilin Dstrict Applied Technology Research and Development Projects in 2022 under Grant No. GX2228. In addition, the research is supported by Open Fund of Key Laboratory of Electronic Equipment Structure Design (Ministry of Education) in Xidian University.

Competing interests. The authors declare no conflicts of interest exist.

Ethical approval. Not applicable.

References

[1] S. Qian, Z. Zhao, P. Qian, Z. Wang and B. Zi, "Research on workspace visual-based continuous switching sliding mode control for cable-driven parallel robots," *Robotica* **42**(1), 1–20 (2024).
[2] M. Khadem, F. Inel, G. Carbone and A. S. T. Tich, "A novel pyramidal cable-driven robot for exercising and rehabilitation of writing tasks," *Robotica* **41**(11), 3463–3484 (2023).
[3] D. Song, M. Lu, L. Zhao, Z. Sun, H. Wang and L. Zhang, "A novel design method for a reconfigurable two-drive cable-driven parallel robot," *Proc. Inst. Mech. Eng. Part C: J. Mech. Eng. Sci.* **239**(6), 2049–2062 (2025).
[4] G. Xu, H. Zhu, H. Xiong and Y. Lou, "Data-driven dynamics modeling and control strategy for a planar n-DOF cable-driven parallel robot driven by n+1 cables allowing collisions," *J. Mech. Robot.* **16**(5), 051008 (2024).
[5] A. M. Barbosa, J. C. M. Carvalho and R. S. Goncalves, "Cable-driven lower limb rehabilitation robot," *J. Braz. Soc. Mech. Sci. Eng.* **40**, 245 (2018).
[6] G. Zuccon, A. Doria, M. Bottin, R. Minto and G. Rosati, "Vibrations of cable-suspended rehabilitation robots," *Robotica* **41**(12), 3702–3723 (2023).
[7] X. Wang, Y. Hu and Q. Lin, "Workspace analysis and verification of cable-driven parallel mechanism for wind tunnel test," *Proc. Inst. Mech. Eng. Part G: J. Aerosp. Eng.* **231**(6), 1012–1021 (2017).
[8] B. Zhang, W. Shang, X. Gao, Z. Li, X. Wang, Y. Ma, F. Zhang, R. Yao, H. Li, J. Yin, Q. Yang and Q. Li, "Synthetic design and analysis of the new feed cabin mechanism in five-hundred-meter aperture spherical radio telescope (FAST)," *Mech. Mach. Theory* **191**, 105507 (2024).
[9] C. Lee and K. Gwak, "Design of a novel cable-driven parallel robot for 3D printing building construction," *Int. J. Adv. Manuf. Technol.* **123**, 4353–4366 (2022).
[10] S. Nguyen-Van and K. Gwak, "A two-nozzle cable-driven parallel robot for 3D printing building construction: Path optimization and vibration analysis," *Int. J. Adv. Manuf. Technol.* **120**, 3325–3338 (2022).
[11] E. Picard, F. Plestan, E. Tahoumi, F. Claveau and S. Caro, "Control strategies for a cable-driven parallel robot with varying payload information," *Mechatronics* **79**(3), 102648 (2021).
[12] S. Behzadipour and A. Khajepour, "Stiffness of cable-based parallel manipulators with application to stability analysis," *ASME J. Mech. Des.* **128**(1), 303–310 (2005).
[13] P. Liu, Y. Qiu, Y. Su and J. Chang, "On the minimum cable tensions for the cable-based parallel robots," *J. Appl. Math.* **2014**(1), 350492 (2014).
[14] P. Bosscher and I. Ebert-Uphoff. "A Stability Measure for Underconstrained Cable-Driven Robots," **In:** *IEEE International Conference on Robotics and Automation, 2004. Proceedings. ICRA '04* (2004) pp. 4943–4949.
[15] P. M. Bosscher. *Disturbance Robustness Measures and Wrench-Feasible Workspace Generation Techniques for Cable-Driven Robots* . Ph.D. Thesis (Georgia Institute of Technology, 2004).
[16] P. Liu, Y. Qiu and Y. Su, "A new hybrid force-position measure approach on the stability for a camera robot," *Proc. Inst. Mech. Eng. Part C: J. Mech. Eng. Sci.* **230**(14), 2508–2516 (2016).
[17] H. Wei, Y. Qiu and J. Yang, "An approach to evaluate stability for cable-based parallel camera robots with hybrid tension-stiffness properties," *Int. J. Adv. Robot. Syst.* **12**, 185 (2015).
[18] Y. Wang, K. Wang, W. Wang, Z. Han and Z. Zhang, "Appraisement and analysis of dynamical stability of under-constrained cable-driven lower-limb rehabilitation training robot," *Robotica* **39**(6), 1023–1036 (2021).
[19] J. Yu, J. Tao, G. Wang, X. Li and H. Wang, "Stability analysis and optimal design of a cable-driven parallel robot," *Robot. Auton. Syst.* **173**, 104611 (2024).
[20] P. Liu, X. Qiao and X. Zhang, "Stability sensitivity for a cable-based coal-gangue picking robot based on grey relational analysis," *Int. J. Adv. Robot. Syst.* **18**(6), 17298814211059729 (2021).
[21] P. Liu, H. Tian, X. Cao, X. Zhang, X. Qiao and Y. Su, "Dynamic stability measurement and grey relational stability sensitivity analysis methods for high-speed long-span 4-1 cable robots," *Mathematics* **10**(24), 4653 (2022).
[22] P. Liu, X. Zhang, X. Qiao and Y. Qiu, "A grey relational analysis method for structural stability sensitivity of cable-suspended camera robots including presence of cable mass," *J. Grey Syst.-UK* **34**(4), 54–77 (2022).
[23] P. Liu, H. Ma, X. Cao, X. Zhang, X. Duan and Z. Nie, "Minimum dynamic cable tension workspace generation techniques and cable tension sensitivity analysis methods for cable-suspended gangue-sorting robots," *Machines* **11**(3), 338 (2023).
[24] P. Liu, H. Tian and X. Qiao, "Minimum cable tensions and tension sensitivity for long-span cable-driven camera robots with applications to stability analysis," *Actuators* **12**(1), 17 (2023).
[25] S. Kim, J. Kim, J. Lee, S. Shim and K. Kim, "Robust optimal design of a neutral valve for hydrostatic transmissions using grey relational analysis," *Proc. Inst. Mech. Eng. Part C: J. Mech. Eng. Sci.* **231**(18), 3414–3428 (2017).

https://doi.org/10.1017/S0263574725102762 Published online by Cambridge University Press

[26] Y. Wang and H. Li, "A novel single-sample retinal vessel segmentation method based on grey relational analysis," *Sensors* **24**(13), 4326 (2024).
[27] C. Gosselin and M. Grenier, "On the determination of the force distribution in overconstrained cable-driven parallel mechanisms," *Meccanica* **46**, 3–15 (2011).
[28] A. Pott, "An Improved Force Distribution Algorithm for Over-Constrained Cable-Driven Parallel Robots," **In:** *Computational Kinematics* (Springer, Heidelberg, 2014) pp. 139–146.
[29] L. Mikelsons, T. Bruckmann, M. Hiller and D. Schramm, "A Real-Time Capable Force Calculation Algorithm for Redundant Tendon-Based Parallel Manipulators," **In:** *2008 IEEE International Conference on Robotics and Automation* (2008) pp. 3869–3874 .
[30] D. Song, M. Lu, L. Zhao, Z. Sun, H. Wang and L. Zhang, "A novel real-time tension distribution method for cable-driven parallel robots," *Robotica* **42**(11), 3692–3708 (2024).
[31] Y. Wang, K. Wang, W. Wang, P. Yin and Z. Han, "Appraise and analysis of dynamical stability of cable-driven lower limb rehabilitation training robot," *J. Mech. Sci. Technol.* **33**(11), 5461–5472 (2019).
[32] E. Ida and M. Carricato, "Static workspace computation for underactuated cable-driven parallel robots," *Mech. Mach. Theory* **193** (2024).
[33] J. Peng, Y. Guo, D. Meng and Y. Han, "Kinematics, statics modeling and workspace analysis of a cable-driven hybrid robot," *Multibody Syst. Dyn.* **61**(2), 163–193 (2024).
[34] Z. Qin, Z. Liu, Y. Liu, H. Gao, C. Sun and G. Sun, "Workspace analysis and optimal design of dual cable-suspended robots for construction," *Mech. Mach. Theory* **171**, 104763 (2022).
[35] H. Liu and Y. Liu, "Colleges' performance assessment of university based on grey relational analysis," *J. Intell. Fuzzy Syst.* **44**(4), 6699–6708 (2023).
[36] F. Sarraf and S. H. Nejad, "Improving performance evaluation based on balanced scorecard with grey relational analysis and data envelopment analysis approaches: Case study in water and wastewater companies," *Eval. Program. Plan.* **79**, 101762 (2020).
[37] S. Singh, I. Singh and A. Dvivedi, "Multi objective optimization in drilling of Al6063/10% SiC metal matrix composite based on grey relational analysis," *Proc. Inst. Mech. Eng. Part B: J. Eng.* **227**(12), 1767–1776 (2013).

Cite this article: P. Liu, X. Duan, Z. Shao and J. Xia (2025). "On the force-pose stability sensitivity analysis method for six-degree-of-freedom spatial cable-suspended parallel robots with eight cables", Robotica **43**, 4040–4063. https://doi.org/10.1017/S0263574725102762

https://doi.org/10.1017/S0263574725102762 Published online by Cambridge University Press